Improved PET Data Quantification in an Integrated Brain MR-PET Scanner

C. Catana[1], T. Benner[1], A. van der Kouwe[1], M. Hamm[2], D. B. Chonde[1], C. J. Michel[2], L. Byars[2], G. El Fakhri[3], N. M. Alpert[3], M. Schmand[2], and A. G. Sorensen[1]

[1]MGH, Radiology, A.A. Martinos Center for Biomedical Imaging, Charlestown, MA, United States, [2]Siemens Healthcare, [3]Radiology, MGH, Division of Nuclear Medicine & Molecular Imaging, United States

INTRODUCTION

Simultaneous MR-PET data acquisition immediately brings to mind the possibility of improving the performance of one instrument by using the information obtained from the other modality. For example, a number of aspects have to be considered in PET for obtaining a correct quantitative measure of the activity concentration in a specific voxel. First, correcting for photon attenuation is essential for quantitative studies. Second, patient motion is difficult to avoid and it leads to degradation (blurring) of PET images and in more severe cases to introduction of artifacts. Third, accurate quantification requires an input function to the kinetic models used for estimating parameters of interest from the dynamic PET data. The accuracy of these methods, in principle, could be improved by including the MR information and we present here our first steps towards achieving these goals.

MATERIALS AND METHODS

Integrated MR-PET Scanner: An MR-compatible brain PET scanner prototype, installed at our site was used for these experiments. This system operates while inserted into the bore of the Siemens 3T TIM Trio MR scanner [1].

MR-based PET attenuation correction: We have previously reported on the importance of accurate bone segmentation for PET attenuation correction [2]. A dual-echo ultra-short echo time (DUTE) sequence was implemented for imaging bone and for deriving the head attenuation map assuming a 3-compartment model (i.e. bone, soft tissue and air) [3].

MR-assisted PET motion correction: A rigid-body motion correction algorithm for the BrainPET scanner was implemented and the results of the first proof-of-principle phantom studies were previously reported [4]. This method was further refined and the first human studies were performed. Three methods were used for MR motion tracking. In the first case, anatomical data were acquired repeatedly during the PET data acquisition using an MPRAGE sequence. Next, cloverleaf navigators embedded in a 3D FLASH sequence were used to obtain motion estimates every TR (i.e. 20 ms) [5]. Finally, motion was tracked every 3 seconds using the standard 3D PACE method [6]. In each case, the rotations and the translations of the object relative to the initial position were calculated.

MR-assisted arterial input function (AIF) estimation: The "gold standard" method for determining the radiotracer AIF is the arterial blood sampling technique. Because this procedure requires catheterization of the radial artery, alternative non-invasive image-based methods have been proposed. In the combined scanner, the anatomical and physiological information provided by the MRI could be used for improving the AIF estimation. As a first step, dynamic PET data were acquired immediately after FDG injection. The listmode data were framed as follows: 12×10s, 2×30s, 2×60s, 2×90s, 2×120s, 1×180s and 2×300s. The PET volumes were reconstructed using a 3D-OSEM algorithm. The major cerebral arteries were segmented from the MR angiography TOF dataset acquired simultaneously. A high-resolution dataset was also acquired using an MPRAGE sequence and structures of interest (i.e. GM, WM, CSF, etc) have been segmented and identified on these images [7]. Average values for all the voxels included in these structures were determined for each of the frames.

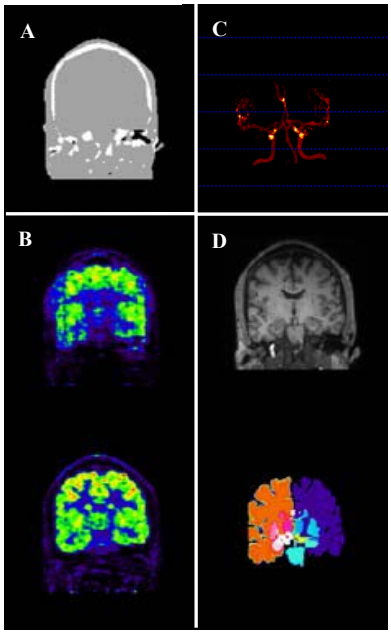

Fig.1: Simultaneous MR-PET data acquisition: (A) μ-map derived from a DUTE MR sequence; (B) PET images before and after MR-assisted motion correction; (C) Cerebral arteries segmented from a TOF sequence; (D) MPRAGE and brain tissues segmentation.

RESULTS AND DISCUSSIONS

MR-based PET attenuation correction: As can be observed in the representative image shown in Fig.1A, most of the soft and bone tissues and air cavities have been correctly identified in the μ-map derived from the DUTE data.

MR-assisted PET motion correction: The images obtained before and after applying the MC are shown in the Fig.1B, demonstrating substantial improvement. Continuous motion tracking during long PET acquisitions will likely require a combination of the various motion tracking approaches proposed. An MR-assisted MC approach has the advantage of guaranteeing the spatial co-registration of the emission and MR-derived attenuation data.

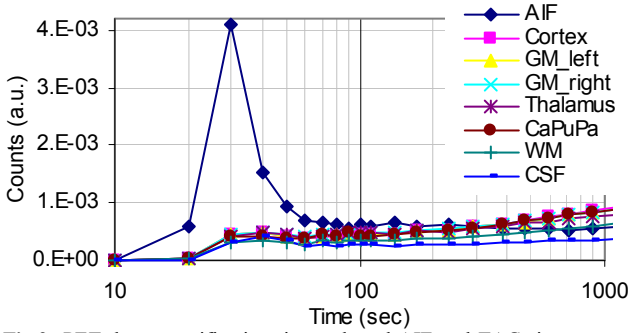

Fig.2: PET data quantification: image-based AIF and TACs in structures of interest segmented from the simultaneously acquired MR data.

MR-assisted radiotracer arterial input function estimation: Using the co-registered MR data, the position of the vessels of interest can be accurately determined (Fig.1C). The image-based AIF and the tissue activity curves plotted as a function of time are shown in Fig.2. As expected, the blood input function peaked in the first minute after injection while the TACs continued to increase even after 25 min. With co-administration of both MR and PET tracers, MR could also provide additional information about the curve (i.e. first 30-60 sec) and any local changes in blood flow, potentially reducing the problems of bolus delay and dispersion inherent in the global AIF estimate. Furthermore, the morphological MR information can be useful for correcting for confounding effects such as spillover from adjacent tissues or partial volume effects in the case of relatively small vessels which can be challenging with only the PET images.

CONCLUSION: As we consider the combination of MR and PET data, from a technical perspective PET might initially appear to benefit more from the addition of simultaneous MR data. In the end, combined MR-PET will likely be a more quantitative tool than the separate modalities, and a number of diseases may yield their secrets best to highly quantitative methods.

REFERENCES: [1] Schlemmer HP et al, Radiol, 2008; 248(3):1028-35; [2] Catana C et al, ISMRM 2009; [3] Catana C et al, ISMRM 2010; [4] Catana C et al, ISMRM 2009; [5] van der Kouwe AJW et al, MRM, 2006; 56: 1019-32; [6] Thesen S et al, MRM, 2000; 44:457-65; [7] Fischl B et al, Neuron, 2002; 33(3): 341-355.